# Rotational Spectrum and Structure of the Carbonyl Sulfide−Trifluoromethane Weakly Bound Dimer

**Michal M. Serafin and Sean A. Peebles***

*Department of Chemistry, Eastern Illinois University, 600 Lincoln Avenue, Charleston, Illinois 61920*

*Received: July 21, 2006; In Final Form: August 31, 2006*

Pure rotational spectra of five isotopomers of the 1:1 weakly bound complex formed between carbonyl sulfide and trifluoromethane (TFM) have been measured using Fourier transform microwave spectroscopy. The experimental rotational constants and dipole moment components are consistent with a structure of $C_s$ symmetry in which the dipole moment vectors of OCS and $HCF_3$ are aligned antiparallel and at an angle of about 40° and with a center of mass separation of 3.965(26) Å. The derived H···O distance is 2.90(5) Å, which is up to 0.6 Å longer than is seen in other similar TFM complexes exhibiting C−H···O interactions. Ab initio calculations at the MP2/6-311++G(2d,2p) level give a structure with rotational constants that are in reasonable agreement with those of the normal isotopic species.

## Introduction

The presence of three electronegative fluorine substituents makes trifluoromethane (TFM) an obvious prototype for the study and quantification of the hydrogen bond donor properties of C−H bonds. In addition, the C−F bonds in $HCF_3$ have also been observed to participate as weak hydrogen bond acceptors, allowing for the formation of triply hydrogen bonded systems such as oxirane−TFM,[1] dioxane−TFM,[2] and cyclobutanone−TFM[3] (in all of which both C−H···O and C−F···H−C interactions are observed).

The OCS−TFM study was motivated by our recent measurements of rotational spectra for several isotopomers of the HCCH−TFM complex.[4] In that case, the assignment was hindered by complicated fine splittings in the spectrum, likely arising from internal motion or torsionally excited states of the TFM monomer. It was hoped that by replacing the nonpolar, symmetric HCCH with a polar, asymmetric OCS subunit, and by the addition of the bulky sulfur atom, the internal motion observed in the HCCH−TFM complex might be reduced; thus, the OCS−TFM system was chosen as a model to help understand the more complex HCCH−TFM dimer. In the case of HCCH−TFM, ab initio calculations at the MP2/6-311++G-(2d,2p) level appeared to provide excellent quantitative predictions for the structure of the dimer, so it was also instructive to test whether the same level of calculation could perform equally well in the case of OCS−TFM.

In previous high-resolution studies of TFM complexes, a range of barriers for the internal rotation of the TFM subunit has been observed. For instance, in the benzene−TFM[5] complex, excited torsional states arising from the nearly free internal rotation of TFM were observed in the spectrum, while in other complexes such as those with oxirane[1] and thiirane,[6] the higher barrier to this internal rotation led to the existence of $A-E$ state spectral splittings, on the order of a few hundred kilohertz. Of course, the triply hydrogen bonded character of many of the previously studied TFM complexes is also expected to contribute to an increase in the barrier height via increased binding interactions.

* Corresponding author. E-mail: sapeebles@eiu.edu. Phone: (217) 581-2679. Fax: (217) 581-6613.

## Experimental Procedures

The rotational spectra of the normal and four singly substituted isotopomers of the OCS−TFM weakly bound complex were measured on a Balle−Flygare Fourier transform microwave spectrometer,[7,8] which is based upon the University of Kiel design.[9] Samples comprising approximately 1% of each gas were condensed into a 2 L glass bulb and diluted to a total pressure of 2−2.5 atm with first-run He/Ne carrier gas (17.5% He/82.5% Ne, BOC Gases). The $O^{13}CS-HCF_3$ ($O^{13}CS$, 99% atom $^{13}C$, Icon Isotopes) and $OCS-DCF_3$ ($DCF_3$ 99.5% atom D, C/D/N Isotopes) spectra were measured using isotopically enriched samples; the other species were measured in natural abundance ($^{13}C$ 1.1% and $^{34}S$ 4.2%). The sample was expanded into the vacuum chamber at a 10 Hz repetition rate via a General Valve Series 9 solenoid valve with a 0.8 mm orifice. Extensive use of Stark effect measurements during our assignment procedure requires the use of a perpendicular expansion to simplify deconvolution of the splitting patterns and so gives rise to a slightly higher full-width at half-maximum value (20−30 kHz) than would be seen with a coaxial expansion. Dipole moment measurements were made by application of electric fields up to ±5 kV to a pair of steel mesh plates located 31 cm apart within the Fabry−Perot cavity. Electric field calibration was carried out using the $J = 1 \leftarrow 0$ transition of carbonyl sulfide and assuming a dipole moment of 0.71521 D.[10]

## Results and Discussion

**Spectra.** The ab initio calculations (to be discussed in the next section) predicted the most stable geometry to be a near-prolate asymmetric top with a $(B + C)$ value of approximately 1.7 GHz. Guided by these predictions, a search in the predicted $J = 4 \leftarrow 3$ region revealed numerous transitions, and the triplet centered around 6417 MHz (consisting of the $K_a = 0$ and $K_a = 1$ components of the $J = 4 \leftarrow 3$ transition) was easily recognized. The predicted value of Ray's asymmetry parameter

10.1021/jp064633x CCC: $33.50 
Published on Web 10/07/2006

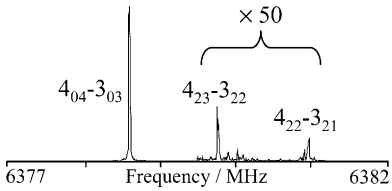


**Figure 1.** Representative portion of the OCS−$DCF_3$ spectrum. The intensity of the $K = 2$ lines has been increased by a factor of 50 since they are considerably weaker than the $K = 0$ line. No resolvable nuclear hyperfine splitting due to the D nucleus can be observed.

($\kappa = -0.985$) for this complex allowed for straightforward location of additional *a* type transitions. The $2_{12} \leftarrow 1_{01}$ *b* type transition was also observed in the initial search region and identified from its Stark effect. Both *a* and *b* type transitions were observed with similar intensity (signal-to-noise values of up to 75 in 50 gas pulses), with optimum microwave pulse lengths consistent with an intermediate sized dipole moment. Some of the transitions were a little broader than would usually be expected, having full-width at half-maximum values of 25−40 kHz, with the lines becoming slightly broader as the transition frequency increased (due to increasing Doppler line widths); no *A*−*E* state splittings due to internal rotation of the trifluoromethane subunit were resolved. The transitions for the OCS−$DCF_3$ species were additionally broadened by unresolved deuterium nuclear quadrupole hyperfine splittings—no attempts were made to assign this hyperfine structure; the $4_{04} \leftarrow 3_{03}$ and the nearby $4_{23} \leftarrow 3_{22}$ and $4_{22} \leftarrow 3_{21}$ transitions for this isotopic species are shown in Figure 1.

Measured transition frequencies were fitted with the SPFIT program of Pickett[11] using the Watson *A* reduced Hamiltonian in the $I^r$ representation.[12] Table 1 lists the measured transitions for the normal isotopomer of OCS−$HCF_3$ along with the residuals ($\Delta\nu = \nu_{obs} - \nu_{calc}$) obtained from the last cycle of the fit. Table 2 lists the fitted spectroscopic constants for the five isotopic species (OCS−$HCF_3$, $O^{13}CS$−$HCF_3$, $OC^{34}S$−$HCF_3$, OCS−$H^{13}CF_3$, and OCS−$DCF_3$). Transition frequencies for the other isotopic species are available as Supporting Information. Note that for the species observed in natural abundance, it was necessary to fix some of the centrifugal distortion constants at those values obtained for the normal isotopomer. The small magnitudes of the distortion constants in the fitted parameters seem to reflect the lack of any significant internal motion perturbations within the spectrum.

**Ab Initio Calculations.** Ab initio calculations were carried out at the MP2/6-311++G(2d,2p) level using Gaussian 03W[13] (for the geometry optimizations) and Gaussian 98[14] (for vibrational frequency calculations) to identify the most stable geometries for the OCS−$HCF_3$ complex and to provide predicted rotational constants to guide the spectral searches. This level of calculation has proven to be helpful in providing reasonable quantitative estimates of the structural parameters of similar complexes at a practical computational cost.[15] The two lowest energy structures obtained from these optimizations are shown in Figure 1, and the important structural and spectroscopic parameters are summarized in Table 3. Both structures exhibit a C−H···O intermolecular interaction and are approximately related by a 60° rotation of the TFM subunit about its $C_3$ axis, although they do differ quite significantly in the other intermolecular parameters (such as the C···C distance; see Table 3). Structure I is predicted to have no imaginary frequencies, while structure II has a single imaginary frequency that corresponds to the torsional motion of the TFM around its $C_3$ axis, moving from structure II toward I. Structure I is predicted to be about 90 $cm^{-1}$ (1.1 kJ $mol^{-1}$) more stable than structure II at the zero-point energy (ZPE) uncorrected level. If ZPE corrections are applied, the energy difference between I and II drops to 70 $cm^{-1}$ (0.8 kJ $mol^{-1}$); both calculations exclude BSSE corrections. Using these energy differences between the two structures as an estimate for the barrier to rotation of the TFM subunit, it is apparent that the value of about 1.1 kJ $mol^{-1}$ (0.8 kJ $mol^{-1}$ ZPE corrected) is somewhat larger than the barriers determined for oxirane−TFM[1] ($V_3$ (expt) = 0.546(4) kJ $mol^{-1}$, $V_3$ (calcd) = 0.72 kJ $mol^{-1}$ (MP2/6-311+G(d, p)), and $V_3$ (calcd) = 0.90 kJ $mol^{-1}$ (MP2/6-311++G(2df, 2p))) and thiirane−TFM[6] ($V_3$ (expt) = 0.526(3) kJ $mol^{-1}$ and $V_3$ (calcd) = 0.91 kJ $mol^{-1}$ (MP2/6-311++G(2df, 2p))). In the TFM complexes with oxirane[1] and thiirane,[6] small (up to a couple hundred kilohertz) *A*−*E* splittings were observed in the rotational spectrum. In light of the calculated values for OCS−$HCF_3$, it seems reasonable to assume small or even unresolvable splittings due to the internal motion of the TFM subunit in the present case. This would be consistent with the observed transitions.

**TABLE 1: Transition Frequencies for the Normal Isotopic Species of the OCS−$HCF_3$ Dimer**

| $J'_{K_aK_c}$ | $J''_{K_aK_c}$ | $\nu_{obs}$ (MHz) | $\nu_{calc}$ (MHz) | $\Delta\nu$ (MHz[a]) |
|---|---|---|---|---|
| $1_{11}$ | $0_{00}$ | 5536.4301 | 5536.4288 | 0.0013 |
| $6_{06}$ | $5_{15}$ | 5850.7024 | 5850.7062 | −0.0038 |
| $4_{14}$ | $3_{13}$ | 6372.0500 | 6372.0462 | 0.0038 |
| $4_{04}$ | $3_{03}$ | 6417.5898 | 6417.5891 | 0.0007 |
| $4_{23}$ | $3_{22}$ | 6418.6059 | 6418.6037 | 0.0022 |
| $4_{32}$ | $3_{31}$ | 6418.9980 | 6418.9997 | −0.0017 |
| $4_{31}$ | $3_{30}$ | 6418.9980 | 6419.0015 | −0.0035 |
| $4_{22}$ | $3_{21}$ | 6419.6442 | 6419.6476 | −0.0034 |
| $4_{13}$ | $3_{12}$ | 6464.8100 | 6464.8100 | 0.0000 |
| $2_{12}$ | $1_{01}$ | 7117.9800 | 7117.9824 | −0.0024 |
| $5_{15}$ | $4_{14}$ | 7964.3752 | 7964.3753 | −0.0001 |
| $5_{05}$ | $4_{04}$ | 8020.6746 | 8020.6782 | −0.0036 |
| $5_{24}$ | $4_{23}$ | 8022.5759 | 8022.5748 | 0.0011 |
| $5_{33}$ | $4_{32}$ | 8023.2972 | 8023.2974 | −0.0002 |
| $5_{32}$ | $4_{31}$ | 8023.2972 | 8023.3038 | −0.0066 |
| $5_{23}$ | $4_{22}$ | 8024.6617 | 8024.6596 | 0.0021 |
| $5_{14}$ | $4_{13}$ | 8080.2250 | 8080.2245 | 0.0005 |
| $3_{13}$ | $2_{02}$ | 8687.8380 | 8687.8424 | −0.0044 |
| $6_{16}$ | $5_{15}$ | 9556.2540 | 9556.2521 | 0.0019 |
| $6_{06}$ | $5_{05}$ | 9622.9004 | 9622.8994 | 0.0010 |
| $6_{25}$ | $5_{24}$ | 9626.0926 | 9626.0935 | −0.0009 |
| $6_{34}$ | $5_{33}$ | 9627.2929 | 9627.2917 | 0.0012 |
| $6_{24}$ | $5_{23}$ | 9629.7374 | 9629.7348 | 0.0027 |
| $6_{15}$ | $5_{14}$ | 9695.1150 | 9695.1130 | 0.0020 |
| $4_{14}$ | $3_{03}$ | 10246.0860 | 10246.0852 | 0.0008 |
| $7_{17}$ | $6_{16}$ | 11147.5879 | 11147.5884 | −0.0005 |
| $7_{07}$ | $6_{06}$ | 11224.0832 | 11224.0837 | −0.0005 |
| $7_{26}$ | $6_{25}$ | 11229.0696 | 11229.0696 | 0.0000 |
| $7_{25}$ | $6_{24}$ | 11234.8845 | 11234.8816 | 0.0029 |
| $7_{16}$ | $6_{15}$ | 11309.3723 | 11309.3694 | 0.0029 |
| $5_{23}$ | $5_{14}$ | 11658.8390 | 11658.8393 | −0.0003 |
| $4_{22}$ | $4_{13}$ | 11714.4020 | 11714.4043 | −0.0023 |
| $5_{15}$ | $4_{04}$ | 11792.8700 | 11792.8714 | −0.0014 |
| $2_{20}$ | $2_{11}$ | 11793.8550 | 11793.8535 | 0.0015 |
| $2_{21}$ | $2_{12}$ | 11863.4114 | 11863.4110 | 0.0004 |
| $3_{22}$ | $3_{13}$ | 11898.3241 | 11898.3274 | −0.0033 |
| $4_{23}$ | $4_{14}$ | 11944.8880 | 11944.8849 | 0.0031 |
| $5_{24}$ | $5_{15}$ | 12003.0855 | 12003.0844 | 0.0011 |
| $6_{25}$ | $6_{16}$ | 12072.9255 | 12072.9258 | −0.0003 |
| $8_{08}$ | $7_{07}$ | 12824.0646 | 12824.0655 | −0.0009 |
| $8_{27}$ | $7_{16}$ | 12831.4129 | 12831.4138 | −0.0009 |
| $8_{26}$ | $7_{25}$ | 12840.1033 | 12840.1057 | −0.0024 |
| $8_{17}$ | $7_{16}$ | 12922.8867 | 12922.8873 | −0.0006 |
| $6_{16}$ | $5_{05}$ | 13328.4477 | 13328.4453 | 0.0024 |

[a] $\Delta\nu = \nu_{obs} - \nu_{calc}$ where $\nu_{calc}$ is calculated from the constants in Table 2.

**Structure.** The similarity of the second moment $P_{cc}$ for the dimer ($P_{cc} = 44.2179(22)$ u Å$^2$) to the $P_{bb}$ moment of the $HCF_3$ monomer ($P_{bb} = 44.57$ u Å$^2$)[16] indicates that two of the fluorine

**TABLE 2: Spectroscopic Constants of the Normal and Isotopically Substituted Species of the OCS−$HCF_3$ Complex**

| parameter | normal | $O^{13}CS-HCF_3$ | $OC^{34}S-HCF_3$ | $OCS-H^{13}CF_3$ | $OCS-DCF_3$ |
|---|---|---|---|---|---|
| $A$ (MHz) | 4745.7148(25) | 4729.2604(25) | 4710.5113(16) | 4744.4633(12) | 4682.6403(32) |
| $B$ (MHz) | 813.9228(27) | 809.7740(5) | 795.1890(8) | 809.8831(7) | 809.7898(4) |
| $C$ (MHz) | 790.9234(27) | 786.5398(4) | 772.2667(7) | 787.0685(4) | 785.3467(5) |
| $\Delta_J$ (kHz) | 2.9352(30) | 2.887(6) | 2.852(8) | 2.907(6) | 2.896(4) |
| $\Delta_{JK}$ (kHz) | −2.032(22) | −2.141(4) | −3.17(21) | −2.032[a] | −2.03(6) |
| $\Delta_K$ (kHz) | 88.8(5) | 88.8(6) | 88.8[a] | 88.8[a] | 87.2(7) |
| $\delta_J$ (kHz) | 0.2817(20) | 0.279(4) | 0.262(7) | 0.284(5) | 0.278(3) |
| $\delta_K$ (kHz) | 57.0(14) | 57.0[a] | 57.0[a] | 57.0[a] | 57.0[a] |
| $N$[b] | 44 | 30 | 15 | 15 | 26 |
| $\Delta\nu_{rms}$ (kHz)[c] | 2.1 | 2.1 | 3.0 | 2.7 | 3.6 |
| $P_{cc}$ (u Å$^2$)[d] | 44.2179(22) | 44.2132(7) | 44.2117(6) | 44.2158(5) | 44.2510(4) |

[a] Some distortion constants were fixed at the value obtained for the normal isotopic species. [b] Number of fitted transitions. [c] $\Delta\nu_{rms} = [\sum(\nu_{obs} - \nu_{calc})^2/N]^{1/2}$. [d] Second moment, $P_{cc} = 0.5(I_a + I_b - I_c)$

**TABLE 3: Comparison of Ab Initio and Experimental Spectroscopic and Structural Parameters for the OCS−$HCF_3$ Dimer**

| | structure I | structure II | experiment | |
|---|---|---|---|---|
| Rotational Constants | | | | |
| $A$ (MHz) | 4637 | 4626 | 4745.7148(25) | |
| $B$ (MHz) | 862 | 727 | 813.9228(27) | |
| $C$ (MHz) | 834 | 707 | 790.9234(27) | |
| Dipole Moment | | | | |
| $\mu_a$ (D) | 0.84 | 1.47 | 0.828(4) | |
| $\mu_b$ (D) | 0.88 | 0.78 | 0.858(7) | |
| $\mu_{total}$ (D) | 1.21 | 1.66 | 1.192(6) | |
| Structure[a] | | | | |
| | | | Inertial | Kraitchman |
| $R$(C···C) (Å) | 3.48 | 3.75 | 3.642(17) | 3.580(2) |
| $\theta$ (deg) | 60.9 | 55.8 | 60.2(1) | 60.5(2) |
| $\phi$ (deg) | 74.8 | 57.3 | 81.1(26) | 83.3(2) |

[a] The experimental structural parameters listed in column 4 are those obtained from a least-squares fit of the 15 isotopic moments of inertia (standard deviation = 0.2915 u Å$^2$; uncertainties reflect one standard deviation), and those listed in column 5 are derived from the Kraitchman single isotopic substitution coordinates for the atoms involved. See text for further discussion.

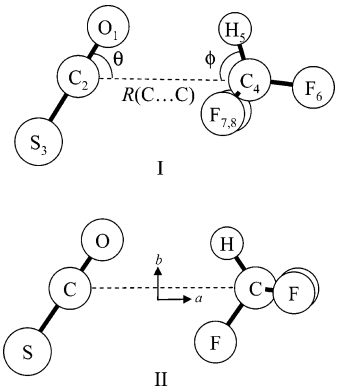


**Figure 2.** Two structures (I and II) obtained from the ab initio optimizations of OCS−$HCF_3$. Structure I has been used to define the three structural parameters needed to describe this complex; the values of these parameters are given in Table 3. The inertial axes for Structure I will be the same as those shown for Structure II.

atoms of the trifluoromethane straddle the *ab* plane of symmetry in the complex. Assuming an *ab* plane of symmetry and with the monomers held fixed at their literature geometries,[16,17] the structure of this dimer may be defined using only three structural parameters ($R$(C···C), $\theta$, and $\phi$—see Figure 2). The experimental moments of inertia from the five isotopic species were least-squares fitted using Schwendeman's STRFITQ program[18] to obtain the values of the three parameters that define the structure of this complex. It should be noted that regardless of whether the out-of-plane fluorine atoms are oriented toward (based on structure I, Figure 2) or away from (based on structure II) the OCS subunit, the same values of $R$(C···C) = 3.642(17) Å, $\theta$ = 60.2(1)°, and $\phi$ = 81.1(26)° result; thus, due to the nonexistence of stable isotopes for fluorine, it is impossible to distinguish spectroscopically between structures I and II. Table 3 compares the experimental structural parameters with those obtained for structures I and II from the ab initio calculations.

**TABLE 4: Kraitchman Single Isotopic Substitution and Inertial Fit Principal Axis Coordinates (in Angstroms)[a]**

| substituted atom | $a$ | $b$ | $c$ |
|---|---|---|---|
| $C_2$ (OCS) | −1.8166 | 0.6005 | 0.0000 |
| | [1.788(1)] | [0.616(3)] | [0.0000] |
| $S_3$ (OCS) | −2.7373 | −0.6652 | 0.0000 |
| | [2.727(1)] | [0.648(2)] | [0.0000] |
| $C_4$ ($HCF_3$) | 1.8044 | 0.2065 | 0.0000 |
| | [1.764(1)] | [0.175(10)] | [0.0000] |
| $H_5$ ($HCF_3$) | 1.7524 | 1.3033 | 0.0000 |
| | [1.770(1)] | [1.187(1)] | [0.190(10)] |

[a] For each substituted atom, the inertial fit coordinate is given first, with the absolute value of the coordinate determined from the Kraitchman single isotopic substitution equations given in brackets. See Figure 2 for atom numbering. Uncertainties in the Kraitchman coordinates are the Costain errors—see text for discussion.

Since single isotopic substitution data are available, it is also possible to obtain an independent determination of the structural parameters from the substitution coordinates derived via the application of Kraitchman's equations.[19,20] Table 4 compares the principal axis coordinates for the singly substituted atoms that result from both the inertial fit and the Kraitchman analysis.[19] In most cases, the agreement is reasonable, with the notable exception of the hydrogen atom. This is unsurprising given the rather large uncertainty (~2.6°) associated with the tilt angle $\phi$ of the trifluoromethane subunit derived from the inertial fit (see Figure 2) and likely reflects the dynamic nature of the TFM subunit as well as highlighting the significant differences in zero-point vibrational motions between the protonated and the deuterated trifluoromethane species.

It is noteworthy that the $P_{cc}$ second moment for the OCS−$DCF_3$ species (Table 2) increases by about 0.04 u Å$^2$ relative to the $HCF_3$-containing isotopomers, perhaps indicating the presence of increased mass out of the symmetry plane during the out-of-plane vibrational motions of the TFM subunit. The derived C═S distance in the OCS monomer subunit using the single substitution principal axis coordinates is 1.574(2) Å (where the quoted uncertainty reflects the Costain error),[21] very close to the monomer literature value of 1.5651 Å.[17] Similarly, the C−H bond distance in $HCF_3$ is determined to be 1.01(10) or 1.03(10) Å, depending on whether the $c$ coordinate of the H atom is assumed to be zero (as expected from the *ab* plane of symmetry) or is taken as given in Table 4, respectively; this value is considerably shorter than the literature value of 1.098

Å.[16] In light of the increased uncertainties in the position of the H atom and the small *b* coordinate of the attached carbon atom, along with the rather large H···O interaction distance, it is highly unlikely that this reflects a significant shortening of this C−H bond; rather, it probably arises from the well-known problems in determining the substitution coordinates for hydrogen.

Using the coordinates in Table 4, it is possible to derive the substitution values of the three structural parameters: $R_s$(C···C) = 3.580(2) Å, $\theta_s = 60.5(2)°$, and $\phi_s = 83.3(2)°$, where the subscript s indicates that these parameters are derived from the single isotopic substitution coordinates (again, the quoted uncertainties reflect the Costain errors[20,21]). The structural parameters obtained from the isotopic substitution data show reasonable agreement with the inertial fit values listed in Table 3, although the substitution C···C distance is some 0.06 Å shorter. The angle $\phi_s$ is also computed to be about 2° larger than the inertial fit value (although it still lies within the experimental uncertainty). This difference may be attributable to the rather small *b* coordinate (0.175 Å) of the carbon atom in the TFM as well as vibrational contamination of the moments for the TFM subunit.

Comparison of the experimental and theoretical structural parameters in Table 3 shows that the fitted *R*(C···C) distance (3.642(17) Å) lies almost exactly halfway between the two distances obtained from ab initio structures I (3.48 Å) and II (3.75 Å). The angular agreement is somewhat less well-reproduced, with the experimental angles $\theta$ and $\phi$ lying closer to the structure I prediction than to that of structure II.

It is also of interest to compare the derived H···O distance in OCS−$HCF_3$ (2.90(5) Å from experimental moment of inertia fits) with similar distances in related TFM complexes. This reveals that in the present case, the H···O interaction is longer by up to 0.6 Å. For instance, in dioxane−TFM, a value of 2.315(85) Å was found,[2] while longer distances of 2.40(1) , 2.42(2), and 2.66(3) Å were obtained for cyclobutanone−TFM,[3] oxirane−TFM,[1] and thiirane−TFM (C−H···S distance),[6] respectively. Of course, in all four of these complexes, additional weak (C−H···F) hydrogen bonding interactions were present, and these will serve to further increase the binding energy and reduce the intermolecular distance.

Using the pseudo-diatomic approximation, it is possible to calculate a value for the stretching force constant ($k_s$) along the weak intermolecular bond via the equation[22]

$$k_s = \frac{16\pi^4(\mu R_{cm})^2[4B^4 + 4C^4 - (B-C)^2(B+C)^2]}{hD_J} \quad (1)$$

where $\mu$ is the pseudo-diatomic reduced mass, $R_{cm}$ is the separation between the centers of mass of the OCS and $HCF_3$ monomers ($R_{cm}$ = 3.965(26) Å), *B* and *C* are the dimer rotational constants, *h* is Planck's constant, and $D_J$ is the Watson *S* reduction distortion constant (which can be calculated easily from the *A* reduction constants). The resulting value of $k_s$ = 1.2(1) N $m^{-1}$ can then be used in the expression $E_B = (1/72)k_s R_{cm}^2$ (obtained from an expansion assuming a Lennard−Jones potential)[23] to estimate a binding energy ($E_B$) for this complex of 1.6(1) kJ $mol^{-1}$. A comparison of this value with binding energies obtained from similar analyses in other TFM complexes is provided in Table 5. This complex has the smallest values of $k_s$ and $E_B$ of the species listed, consistent with the considerably longer H···O distance as discussed earlier. Again, this weaker binding is consistent with the absence of the additional C−F···H−C hydrogen bonding interactions that were possible in the oxirane,[1] dioxane,[2] cyclobutanone,[3] and thiirane[6] complexes with TFM. Interestingly, the benzene−TFM complex,[5] which is bound only by a C−H···$\pi$ interaction, has a binding energy that lies among the more strongly bound of the complexes listed (Table 5).

**TABLE 5: Comparison of Derived Force Constants and Binding Energies for Other Trifluoromethane Complexes**

| | $k_s$ (N $m^{-1}$) | $E_B$ (kJ $mol^{-1}$) | ref |
|---|---|---|---|
| OCS | 1.2(1) | 1.6(1) | *a* |
| Cyclobutanone | 4.8 | 2.5 | 3 |
| Dioxane | 5.0 | 6.8 | 2 |
| Oxirane | 6.0 | 6.7 | 1 |
| Benzene | 6.8 | 8.4 | 5 |
| Thiirane | 7.2[b] | 9.8 | 6 |

[a] This paper. [b] Calculated from the value of $E_B$ and other parameters tabulated in ref 6.

**TABLE 6: Dipole Moment Data for the OCS−$HCF_3$ Complex[a]**

| transition | \|*M*\| | $\Delta\nu/E^2$ (obs) | $\Delta\nu/E^2$ (calcd)[b] | % difference |
|---|---|---|---|---|
| $1_{10} \leftarrow 0_{00}$ | 0 | 6.2352 | 6.2544 | −0.3 |
| $2_{12} \leftarrow 1_{01}$ | 0 | −2.9112 | −2.8067 | 3.6 |
| | 1 | −5.5862 | −5.6399 | −1.0 |
| $3_{13} \leftarrow 2_{02}$ | 1 | 0.5218 | 0.5060 | 3.0 |
| | 2 | −1.8410 | −1.7899 | 2.8 |
| $4_{14} \leftarrow 3_{13}$ | 1 | 0.8491 | 0.8127 | 4.3 |
| | | $\mu_a$ = 0.828(4) D | | |
| | | $\mu_b$ = 0.858(7) D | | |
| | | $\mu_{total}$ = 1.192(6) D | | |

[a] Observed and calculated Stark coefficients are in units of $10^{-5}$ MHz $V^{-2}$ $cm^2$. [b] Calculated Stark coefficients are computed from second-order perturbation theory using the rotational constants given in Table 2.

**Dipole Moment.** Measured Stark coefficients for six Stark lobes from four rotational transitions were least-squares fitted[24] to obtain the two components of dipole moment for OCS−TFM. Since this complex contains an *ab* plane of symmetry, a zero $\mu_c$ component of the dipole moment was expected and indeed was obtained. Table 6 compares the observed and calculated[25] Stark coefficients (determined via second-order perturbation theory using the rotational constants in Table 2) and also lists the experimental dipole moment components.

Projection of the individual monomer dipole moments ($\mu_{OCS}$ = 0.71521 D[10] and $\mu_{TFM}$ = 1.65 D[26]) into the principal axis frame of the dimer (based on the structure obtained from the inertial fit) gives $\mu_a$ = 0.50 D and $\mu_b$ = 1.07 D and a total dipole moment $\mu_{total}$ = 1.18 D. The experimentally determined dipole moment ($\mu_a$ = 0.828(4) D, $\mu_b$ = 0.858(7) D, $\mu_{total}$ = 1.192(6) D) shows an increase in the $\mu_a$ component and a decrease in the $\mu_b$ component by roughly the same amount (∼0.3 D) relative to the projected moments.

To explore the magnitude of induced dipole moments upon formation of the complex and hence to attempt to rationalize the difference between projected and experimental moments, geometry optimizations employing Stone's Orient model[27] were carried out, both including and neglecting induction contributions to the overall interaction energy. Details of the Orient model have been given previously,[28] and so only brief details of the calculations will be given here. The charge distribution of each monomer was described using distributed multipole analyses (DMAs) calculated with the GDMA program[29] (which uses formatted checkpoint files from Gaussian 03W;[13] these DMAs were calculated from MP2/6-311++G(2d,2p) wave functions). Atom−atom dispersion and repulsion parameters were obtained from Mirsky's tabulations,[30,31] and for the calculations including induction, molecular polarizabilities for

**TABLE 7: Comparison of Dipole Moment Components for the OCS−TFM Complex**

| source | $\mu_a$ (D) | $\mu_b$ (D) |
|---|---|---|
| projected[a] | 0.50 | 1.07 |
| experimental | 0.828(4) | 0.858(7) |
| orient (no induction) | 0.76 | 1.12 |
| orient (with induction) | 0.91 | 0.94 |

[a] Calculated by projection of the literature monomer dipole moments into the principal axis system of the experimentally determined (inertial fit) structure.

OCS[32] and TFM[33] were placed at the center of mass of each molecule. The induction energy and induced moments were then iterated to convergence during the geometry optimization. The Orient results are summarized in Table 7, and it can be seen that the induced moments behave in the correct sense—inclusion of the induction contributions in the Orient model increases the $\mu_a$ dipole component by about 0.15 D and decreases $\mu_b$ by 0.18 D relative to the calculations without induction. These changes are of a somewhat smaller magnitude than is seen experimentally but are in the right sense and are of roughly equal magnitude. It should be noted that the structures (obtained with and without induction) that result from calculations using the default parameters in Orient differ only slightly (with no induction: $R$(C···C) = 3.68 Å, $\theta = 54.8°$, and $\phi = 74.9°$; with induction: $R$(C···C) = 3.66 Å, $\theta = 55.4°$, and $\phi = 73.5°$—both are in remarkably good agreement with the experimental structure), but these structural differences are too small to have a significant effect on the values of the dipole moments.

Finally, a comparison of the experimental and MP2/6-311++G(2d,2p) predicted dipole moments (Table 3) reveals that the dipole moment components for structure I ($\mu_a = 0.84$ D and $\mu_b = 0.88$ D) are in excellent agreement with the experimental values, while those of structure II ($\mu_a = 1.47$ D and $\mu_b = 0.78$ D) are significantly further away.

## Conclusion

Rotational constants for five isotopomers of the trifluoromethane−OCS complex have been used to determine a structure of $C_s$ symmetry that is in reasonable agreement with predictions from ab initio optimizations at the MP2/6-311++G(2d,2p) level and semiempirical calculations using the Orient model. The C···C intermolecular bond distance of 3.642(17) Å lies almost equidistant between the two ab initio structures, which have the fluorine atoms that straddle the symmetry plane either pointing toward or away from the OCS monomer. Relatively large uncertainties in the tilt angle of the TFM subunit (∼3°) may be attributable to some torsional motion of this monomer, although with a sufficiently large barrier that the $A-E$ splittings are unresolved in the rotational spectrum.

**Acknowledgment.** The authors acknowledge the donors of the ACS Petroleum Research Fund (PRF 39752-GB6) for support of this work. We also thank Dr. Rebecca Peebles for many useful discussions and for suggestions during the preparation of the manuscript.

**Supporting Information Available:** Tables of measured transition frequencies for the four isotopic species. This material is available free of charge via the Internet at http://pubs.acs.org.

## References and Notes

(1) Alonso, J. L.; Antolínez, S.; Blanco, S.; Lesarri, A.; López, J. C.; Caminati, W. *J. Am. Chem. Soc.* **2004**, *126*, 3244.

(2) Favero, L. B.; Giuliano, B. M.; Melandri, S.; Maris, A.; Ottaviani, P.; Velino, B.; Caminati, W. *J. Phys. Chem. A* **2005**, *109*, 7402.

(3) Ottaviani, P.; Caminati, W.; Favero, L. B.; Blanco, S.; López, J. C.; Alonso, J. L. *Chem.—Eur. J.* **2006**, *12*, 915.

(4) Serafin, M. M.; Peebles, R. A.; Peebles, S. A. **2006**, unpublished observations.

(5) López, J. C.; Caminati, W.; Alonso, J. L. *Angew. Chem., Int. Ed.* **2005**, *45*, 290.

(6) Cocinero, E. J.; Sanchez, R.; Blanco, S.; Lesarri, A.; López, J. C.; Alonso, J. L. *Chem. Phys. Lett.* **2005**, *402*, 4.

(7) Balle, T. J.; Flygare, W. H. *Rev. Sci. Instrum.* **1981**, *52*, 33.

(8) Newby, J. J.; Serafin, M. M.; Peebles, R. A.; Peebles, S. A. *Phys. Chem. Chem. Phys.* **2005**, *7*, 487.

(9) Grabow, J.-U. Ph.D. Thesis, University of Kiel, Kiel, Germany, 1992.

(10) Muenter, J. S. *J. Chem. Phys.* **1968**, *48*, 4544.

(11) Pickett, H. M. *J. Mol. Spectrosc.* **1991**, *148*, 371.

(12) Watson, J. K. G. *Vib. Spectra Struct.* **1977**, *6*, 1.

(13) Frisch, M. J.; Trucks, G. W.; Schlegel, H. B.; Scuseria, G. E.; Robb, M. A.; Cheeseman, J. R.; Montgomery, J. A., Jr.; Vreven, T.; Kudin, K. N.; Burant, J. C.; Millam, J. M.; Iyengar, S. S.; Tomasi, J.; Barone, V.; Mennucci, B.; Cossi, M.; Scalmani, G.; Rega, N.; Petersson, G. A.; Nakatsuji, H.; Hada, M.; Ehara, M.; Toyota, K.; Fukuda, R.; Hasegawa, J.; Ishida, M.; Nakajima, T.; Honda, Y.; Kitao, O.; Nakai, H.; Klene, M.; Li, X.; Knox, J. E.; Hratchian, H. P.; Cross, J. B.; Bakken, V.; Adamo, C.; Jaramillo, J.; Gomperts, R.; Stratmann, R. E.; Yazyev, O.; Austin, A. J.; Cammi, R.; Pomelli, C.; Ochterski, J. W.; Ayala, P. Y.; Morokuma, K.; Voth, G. A.; Salvador, P.; Dannenberg, J. J.; Zakrzewski, V. G.; Dapprich, S.; Daniels, A. D.; Strain, M. C.; Farkas, O.; Malick, D. K.; Rabuck, A. D.; Raghavachari, K.; Foresman, J. B.; Ortiz, J. V.; Cui, Q.; Baboul, A. G.; Clifford, S.; Cioslowski, J.; Stefanov, B. B.; Liu, G.; Liashenko, A.; Piskorz, P.; Komaromi, I.; Martin, R. L.; Fox, D. J.; Keith, T.; Al-Laham, M. A.; Peng, C. Y.; Nanayakkara, A.; Challacombe, M.; Gill, P. M. W.; Johnson, B.; Chen, W.; Wong, M. W.; Gonzalez, C.; Pople, J. A.; Gaussian 03W, revision D.01; Gaussian, Inc.: Pittsburgh, PA, 2004.

(14) Frisch, M. J.; Trucks, G. W.; Schlegel, H. B.; Scuseria, G. E.; Robb, M. A.; Cheeseman, J. R.; Zakrzewski, V. G.; Montgomery, J. A., Jr.; Stratmann, R. E.; Burant, J. C.; Dapprich, S.; Millam, J. M.; Daniels, A. D.; Kudin, K. N.; Strain, M. C.; Farkas, O.; Tomasi, J.; Barone, V.; Cossi, M.; Cammi, R.; Mennucci, B.; Pomelli, C.; Adamo, C.; Clifford, S.; Ochterski, J.; Petersson, G. A.; Ayala, P. Y.; Cui, Q.; Morokuma, K.; Malick, D. K.; Rabuck, A. D.; Raghavachari, K.; Foresman, J. B.; Cioslowski, J.; Ortiz, J. V.; Stefanov, B. B.; Liu, G.; Liashenko, A.; Piskorz, P.; Komaromi, I.; Gomperts, R.; Martin, R. L.; Fox, D. J.; Keith, T.; Al-Laham, M. A.; Peng, C. Y.; Nanayakkara, A.; Gonzalez, C.; Challacombe, M.; Gill, P. M. W.; Johnson, B. G.; Chen, W.; Wong, M. W.; Andres, J. L.; Head-Gordon, M.; Replogle, E. S.; Pople, J. A. Gaussian 98, Revision A.9; Gaussian, Inc., Pittsburgh, PA, 1998.

(15) See, for example, Newby, J. J.; Peebles, R. A.; Peebles, S. A. *J. Phys. Chem. A* **2004**, *108*, 7372. Newby, J. J.; Peebles, R. A.; Peebles, S. A. *J. Phys. Chem. A* **2004**, *108*, 11234.

(16) Ghosh, S.; Trambarulo, R.; Gordy, W. *J. Chem. Phys.* **1952**, *20*, 605.

(17) Harmony, M. D.; Laurie, V. W.; Kuczkowski, R. L.; Schwendeman, R. H.; Ramsay, D. A.; Lovas, F. J.; Lafferty, W. J.; Maki, A. J. *J. Phys. Chem. Ref. Data* **1979**, *8*, 619.

(18) Schwendeman, R. H. In *Critical Evaluation of Chemical and Physical Structural Information*; Lide, D. R., Paul, M. A., Eds.; National Academy of Sciences: Washington, DC, 1974. The STRFITQ program used in this work is the University of Michigan modified version of Schwendeman's original code.

(19) Kraitchman, J. *Am. J. Phys.* **1953**, *21*, 17.

(20) Kraitchman coordinates and propagated errors in parameters calculated using the KRA and EVAL code, Kisiel, Z. PROSPE−Programs for Rotational Spectroscopy; http://info.ifpan.edu.pl/∼kisiel/prospe.htm, accessed July 2006.

(21) Costain, C. C. *Trans. Am. Crystallogr. Assoc.* **1966**, *2*, 157.

(22) Millen, D. J. *Can. J. Chem.* **1985**, *63*, 1477.

(23) Read, W. G.; Campbell, E. J.; Henderson, G. *J. Chem. Phys.* **1983**, *78*, 3501.

(24) Dipole moment components were fitted using the program *DIPFIT*, Hillig, K. W.; University of Michigan: Ann Arbor, MI.

(25) Stark coefficients were calculated using a modified version of the original ASYSPEC code: Beaudet, R. A. Ph.D. Thesis, Harvard University, Cambridge, MA, 1961.

(26) Nelson, R. D.; Lide, D. R.; Maryott, A. A. In *Selected Values of Electric Dipole Moments for Molecules in the Gas Phase*; NIST Standard Reference Database, NBS10: Washington, DC, 1967.

(27) Stone, A. J.; Dullweber, A.; Engkvist, O.; Fraschini, E.; Hodges, M. P.; Meredith, A. W.; Nutt, D. R.; Popelier, P. L. A.; Wales, D. J. *Orient: A Program for Studying Interactions between Molecules*, version

4.5; University of Cambridge: Cambridge, UK, 2002. Enquiries to A. J. Stone, ajs1@cam.ac.uk

(28) Peebles, S. A.; Kuczkowski, R. L. *J. Mol. Struct.* **1998**, *447*, 151.

(29) Stone, A. J. *J. Chem. Theory Comput.* **2005**, *1*, 1128; http://dx.doi.org/10.1021/ct050190+.

(30) Stone, A. J. *The Theory of Intermolecular Forces, International Series of Monographs in Chemistry*; Clarendon Press: Oxford, 1996.

(31) Mirsky, K. The determination of the intermolecular interaction energy by empirical methods. In *Computing in Crystallography*; Schenk, R., Olthof-Hazenkamp, R., van Koningsveld, H., Bassi, G. C., Eds.; Delft University Press: Delft, The Netherlands, 1978; p 169.

(32) Gray, C. G.; Gubbins, K. E. *Theory of Molecular Fluids, Vol. 1, Fundamentals*; Oxford University Press: Oxford, UK, 1984.

(33) Le Fevre, R. J. W.; Ritchie, G. L. D. *J. Chem. Soc.* **1965**, 3520.